Received: 8 September 2023 | Revised: 7 December 2023 | Accepted: 7 January 2024

DOI: 10.1111/pce.14821

ORIGINAL ARTICLE

Plant, Cell & Environment | PC&E | WILEY

Stomatal conductance reduction tradeoffs in maize leaves: A theoretical study

Antriksh Srivastava[1] | **Venkatraman Srinivasan**[1,2] | **Stephen P. Long**[3,4,5,6]

[1]Department of Civil Engineering, Indian Institute of Technology Madras, Chennai, India

[2]School of Sustainability, Indian Institute of Technology Madras, Chennai, India

[3]The Carl R. Woese Institute for Genomic Biology, University of Illinois at Urbana Champaign, Champaign, Illinois, USA

[4]Department of Crop Sciences, University of Illinois Urbana Champaign, Champaign, Illinois, USA

[5]Department of Plant Biology, University of Illinois Urbana Champaign, Champaign, Illinois, USA

[6]Lancaster Environment Centre, Lancaster University, Lancaster, UK

Correspondence
Venkatraman Srinivasan, Department of Civil Engineering, Indian Institute of Technology Madras, Chennai, India.
Email: venkatraman@iitm.ac.in

Funding information
Foundation for Food and Agriculture Research (FFAR) and the UK Foreign, Commonwealth and Development Office, Grant/Award Number: OPP1172157; Center for Industrial Consultancy and Sponsored Research, Indian Institute of Technology Madras, Grant/Award Numbers: CIE1819847NFIGVENT, CE1920364NFSC008930; Prime Minister's Research Fellowship from the Department of Science and Technology, India, Grant/Award Number: SB22230182CEPMRF008930; Science and Engineering Research Board, Department of Science and Technology, India, Grant/Award Number: ECR2018002762; Realizing Increased Photosynthetic Efficiency (RIPE) from the Bill & Melinda Gates Foundation

Abstract

As the leading global grain crop, maize significantly impacts agricultural water usage. Presently, photosynthesis (A_{net}) in leaves of modern maize crops is saturated with CO_2, implying that reducing stomatal conductance (g_s) would not affect A_{net} but reduce transpiration (τ), thereby increasing water use efficiency (WUE). While g_s reduction benefits upper canopy leaves under optimal conditions, the tradeoffs in low light and nitrogen-deficient leaves under nonoptimal microenvironments remain unexplored. Moreover, g_s reduction increases leaf temperature (T_{leaf}) and water vapor pressure deficit, partially counteracting transpiratory water savings. Therefore, the overall impact of g_s reduction on water savings remains unclear. Here, we use a process-based leaf model to investigate the benefits of reduced g_s in maize leaves under different microenvironments. Our findings show that increases in T_{leaf} due to g_s reduction can diminish WUE gains by up to 20%. However, g_s reduction still results in beneficial WUE tradeoffs, where a 29% decrease in g_s in upper canopy leaves results in a 28% WUE gain without loss in A_{net}. Lower canopy leaves exhibit superior tradeoffs in g_s reduction with 178% gains in WUE without loss in A_{net}. Our simulations show that these WUE benefits are resilient to climate change.

KEYWORDS
C4 plants, climate change, crop optimization, stomatal conductance, water use efficiency

1 | INTRODUCTION

The United Nations FAO has predicted that food production must increase by 60%–100% in 2050 to meet the demands of a growing population (FAO et al., 2021; Tilman & Clark, 2015). This increase has to be accomplished under the threat of climate change with higher air temperatures (T_{air}) and water vapor pressure deficits (VPD), which increase crop water demand (Lobell et al., 2013; Yuan et al., 2019). While improvements in genetics and agronomy have resulted in a near-linear increase in crop yield per hectare over the past 60 years, the water required per biomass unit has stayed the same (Lobell et al., 2014; Ort & Long, 2014). Therefore, increased crop yields have inadvertently increased agricultural water use (Lobell et al., 2013, 2014; Ort & Long, 2014). Agriculture consumes nearly 70% of the world's freshwater resources (UNESCO, 2001). While only 17% of global cropland is irrigated, mainly through unsustainable

means, it accounts for nearly 30% of worldwide food production (Nagaraj et al., 2021). Furthermore, due to predicted increases in the intensity and frequency of droughts (IPCC, 2014), the water available to grow these crops will continue to decline (Chan et al., 2021; IPCC, 2014), posing significant challenges to achieving future yield targets. In this context, strategies for increasing crop yields while conserving water must be addressed along with crop improvement (Drewry et al., 2014; Lawson & Matthews, 2020; Long et al., 2022; Srinivasan et al., 2016).

Stomata are specialized cell complexes on the leaf epidermis, which regulate the uptake of CO_2 into the leaf's internal air space for carbon assimilation, thereby exposing the wet surfaces of leaf cells to the atmosphere (Cowan & Farquhar, 1977; Lawson & Matthews, 2020). Photosynthetic assimilation (A_{net}) and transpiration (τ) rates are therefore determined by stomatal conductance (g_s), which depends on the stomatal number, morphology, and aperture (Hetherington & Woodward, 2003; Lawson & Blatt, 2014; Lawson et al., 2011). An inherent aspect of plant growth is the trade-off between net photosynthetic carbon assimilation and transpiratory water loss (Faralli et al., 2019; Franks & Farquhar, 2007; Lawson & Blatt, 2014). Water use efficiency (WUE) is the amount of carbon gained per unit of water lost. For a given leaf microenvironment, the WUE of C_4 leaves is higher than that of C_3 leaves. This is because phospho-enol pyruvate (PEP) carboxylase acts as the primary carboxylase and the effective absence of photorespiration resulting in a lower intercellular [CO_2] (C_i) during photosynthesis, typically around 55% of that in C_3 leaves (Hatch, 1987; von Caemmerer, 2000). This steeper gradient of [CO_2] between the leaf surface and intercellular space allows the C_4 leaf to assimilate more CO_2 for any given stomatal conductance, resulting in a higher leaf-level WUE.

When exposed to high incident light, leaves of C_4 crops like maize show a biphasic response of A_{net} to C_i (A-Ci response). This response is characterized by an initial steep increase in A_{net} resulting from the activity of PEP carboxylase followed by a sharp inflection to a plateau determined by rubisco activity, the rate of PEP regeneration, or an electron transport limitation (von Caemmerer & Furbank, 1999). The C_i occurring under a given atmospheric [CO_2] is the operating C_i, and the corresponding A_{net} at which it occurs is the operating point (Farquhar & Sharkey, 1982). The supply function is the line connecting the operating point on the A-Ci response to the corresponding atmospheric [CO_2] on the x-axis ($A_{net} = 0$). The slope of this supply function gives the magnitude of total conductance (g) (harmonic mean of stomatal conductance and boundary layer conductance). This slope decreases at higher atmospheric [CO_2], due to a drop in g_s (Leakey et al., 2006; Maherali et al., 2002; Pignon & Long, 2020).

A meta-analysis of A-Ci responses of C_4 plants showed that, at current atmospheric [CO_2] (C_a), the operating point for maize leaves is on the plateau region, that is, A_{net} is [CO_2] saturated (Pignon & Long, 2020). Therefore, g_s could be reduced at the current atmospheric [CO_2], lowering C_i without affecting A_{net} while improving WUE by decreasing τ. Under a future elevated [CO_2], the operating point shifts further into the plateau region of the A-Ci response (Leakey et al., 2006), enabling even greater g_s reductions with additional improvements in WUE. Today, there are several bioengineering strategies to reduce g_s, while variation in g_s within crop germplasm may allow breeding for decreased g_s (Faralli et al., 2019; Long et al., 2022; Phetluan et al., 2023; Pitaloka et al., 2022).

Would such a reduction in g_s result in lower overall crop water use and be worthwhile? The benefits of g_s reduction may be valid for upper canopy leaves receiving full sunlight on a clear-sky day around solar noon under ideal leaf microenvironmental conditions. However, the tradeoffs for g_s reduction under low light, low leaf nitrogen, and nonoptimal leaf canopy microenvironmental conditions are not well explored. For example, during periods of low solar zenith angles (mornings and evenings) or under cloudy sky conditions, incident light levels of upper canopy leaves are much lower. Additionally, lower canopy leaves operate at lower light levels throughout the day as they are mostly shaded (Campbell & Norman, 1998; Collison et al., 2020; Srinivasan et al., 2016). Shaded leaves of modern maize cultivars typically constitute up to 60% of the total crop leaf area and contribute up to 35% of carbon uptake and 54% of water use (Drewry et al., 2010). At lower light levels, photosynthetic rates are smaller and are typically energy-limited, where the advantage of the carbon concentrating mechanism may be diminished (Farquhar & Sharkey, 1982; Pignon et al., 2017; von Caemmerer, 2000). The g_s of shaded leaves is lower than that of sunlit leaves (Farquhar & Sharkey, 1982; Pearcy, 1990), and whether further g_s reduction would result in beneficial tradeoffs is unknown. Also, lower canopy leaves have reduced nitrogen content, hence, lower photosynthetic capacities (Leuning et al., 1995; Morgan et al., 2004). The A-Ci response of C_4 leaves with lower photosynthetic capacities plateaus at lower A_{net} values (Marchiori et al., 2014). The g_s reduction tradeoffs in C_4 leaves with lower photosynthetic capacities are yet to be fully explored.

Atmospheric relative humidity (RH) significantly impacts the operating point of C_4 leaves. Over a typical diurnal period in the US corn belt, RH and VPD vary between 50%–100% and 3–0 kPa, respectively (Drewry et al., 2010; Kimm et al., 2020). g_s decreases under higher VPD (Grossiord et al., 2020; Sulman et al., 2016), shifting the operating point towards the initial slope of the A-Ci response. A further reduction in g_s under a high VPD could result in undesirable WUE tradeoffs if the operating point transitions to the initial slope of the A-Ci response. Climate change is projected to exacerbate this problem as VPD increases in the future (DeLucia et al., 2019; Lobell et al., 2014; Pryor & Barthelmie, 2013), further diminishing the potential for g_s reduction. A systematic analysis of the tradeoffs of g_s reduction under higher VPD is currently lacking.

A reduction in τ results in a reduced latent heat cooling, inducing an increase in leaf temperature (T_{leaf}) and sensible heat through energy balance feedback (Figure 1). Higher T_{leaf} increases VPD, reducing g_s. This T_{leaf} increase-driven g_s reduction has the potential to cause undesirable declines in A_{net} (Figure 1). Increases in T_{leaf} also directly impact A_{net} (Figure 1) by altering the enzyme kinetics of photosynthetic parameters, depending on the optimum temperature for photosynthesis (Lobell et al., 2013; Massad et al., 2007). Furthermore, the leaf boundary layer conductance (g_b), which is influenced by the temperature difference between the leaf and its microenvironment, can potentially increase under elevated T_{leaf}

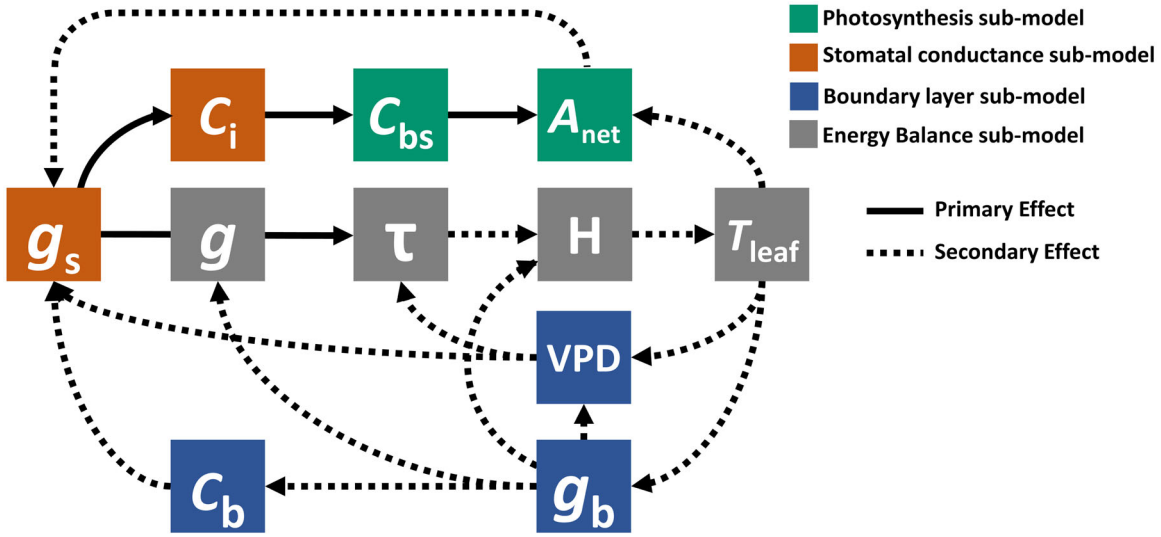

FIGURE 1 Conceptual illustration of g_s reduction's primary and secondary effects on leaf-level transpiration (τ) and photosynthesis (A_{net}). g_b is the boundary layer conductance, C_{bs} is the bundle sheath [CO_2], C_b is the boundary layer [CO_2], and H is the sensible heat flux. [Color figure can be viewed at wileyonlinelibrary.com]

(Nikolov et al., 1995). We term these T_{leaf} increase-induced energy-balance feedbacks as secondary effects. The extent to which τ savings from g_s reductions are diminished by the secondary feedback of increased T_{leaf} and its impact on the overall leaf WUE has not been sufficiently investigated.

In this paper, we test the hypothesis that decreasing g_s in maize leaves results in significant increases in WUE without loss of photosynthetic carbon uptake under varying leaf microenvironmental conditions. This is accomplished through model simulations using an integrated, process-based, semimechanistic, C_4 leaf model (vLeaf) that couples (i) a biophysical model for photosynthesis (von Caemmerer, 2000), (ii) an empirical model of stomatal conductance (Leuning, 1990), (iii) leaf-boundary layer conductance model (Nikolov et al., 1995), and (iv) a leaf-energy balance model (Drewry et al., 2010; Nikolov et al., 1995). Through model simulations, we quantify the tradeoffs in genetic g_s reduction under varying (i) atmospheric [CO_2], (ii) incident light, (iii) atmospheric humidity, (iv) leaf nitrogen content, and (v) T_{air}. Using a set of modified energy-balance simulations, we isolate and quantify the effect of g_s reduction on the altered energy balance and its impact on WUE. Using model simulations, we estimate the g_s reduction tradeoffs between loss in A_{net} versus savings in τ under current and projected future climatic conditions and identify the corresponding optimal g_s reduction potentials.

2 | METHODS

2.1 | C_4 leaf model

A steady-state C_4 leaf model (vLeaf) was developed to simulate leaf response under various microenvironmental conditions (Figure 2). vLeaf models the fluxes of CO_2 from the leaf microenvironment through the boundary layer, leaf intercellular space, carbon concentration mechanism in the mesophyll cell, and finally, to the bundle sheath chloroplast site where subsequent CO_2 fixation occurs. It also models the water vapor fluxes from the leaf intercellular space to the leaf microenvironment through the leaf boundary layer and the sensible heat flux from the leaf surface to the surrounding microenvironment. vLeaf couples four submodels: (i) photosynthesis (Section S1.1), (ii) stomatal conductance (Section S1.2), (iii) boundary layer (Section S1.3), and (iv) energy balance (Section S1.4). A brief outline of vLeaf and its submodels is given below. The supporting Information materials (Section S1) present full details, including equations and parameters.

The photosynthesis submodel computes the net carbon flux (A_{net}) based on the von Caemmerer (2000) model for C_4 photosynthesis. The model assumes photosynthesis is either limited by PEP carboxylation rates at the mesophyll cells (A_p) or Rubisco carboxylation rates at the bundle sheath cells (A_c). A_p and A_c can, in turn, be either energy-limited or CO_2-limited based on the input C_i (obtained from the stomatal conductance submodel), absorbed PAR, and photosynthetic enzyme concentrations. The model accounts for (i) photorespiration in the bundle sheath cells, (ii) dark respiration in the bundle sheath and mesophyll cells, and (iii) diffusive leakage of CO_2 from the bundle sheath to the mesophyll cells. The temperature dependence of enzyme kinetics is modeled through temperature-response functions using the T_{leaf} values obtained from the energy balance submodel (Chen et al., 1994; Massad et al., 2007).

The stomatal conductance submodel computes g_s using the empirical modified Ball-Berry formulation (Ball et al., 1987) that accounts for the CO_2 compensation point (Leuning, 1990). g_s is computed using A_{net} obtained from the photosynthesis submodel, and the boundary layer (leaf surface) concentrations of water vapor (e_b) and CO_2 (C_b) are obtained from the boundary layer submodel. C_i

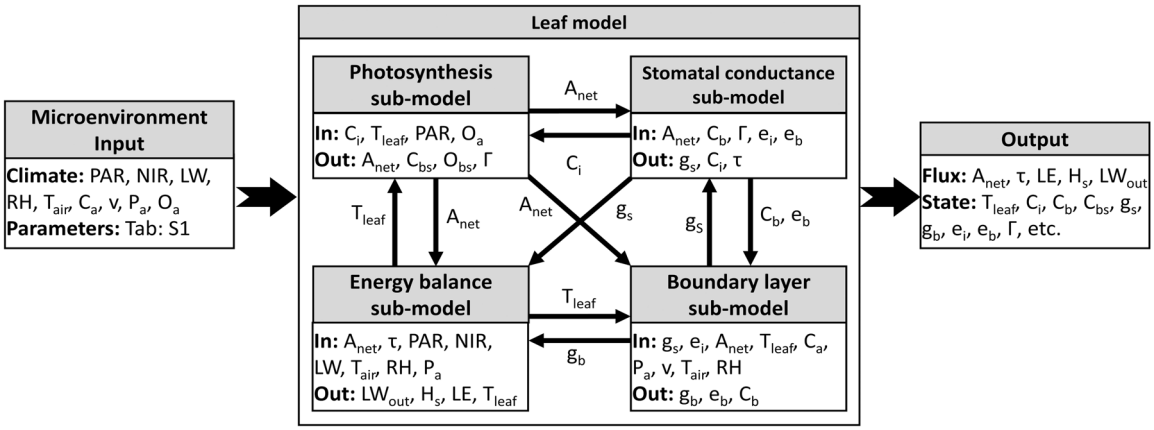

FIGURE 2 Interconnectivity of submodels involved in the C_4 leaf model (vLeaf). Arrows connect the submodels using variables (written alongside arrows) from one submodel's output to another submodel's input.

and τ are computed using steady-state mass-balance equations from g_s, C_b, e_b, and A_{net}. The stomatal conductance submodel does not account for the effect of water stress on g_s.

The boundary layer submodel computes g_b based on the formulation given by Nikolov et al. (1995). The model accounts for conductance limitations due to free convection ($g_{b,free}$) caused by thermal gradients between the leaf surface and the microenvironment (using T_{leaf} from the energy-balance submodel) or forced convection ($g_{b,forced}$) driven by wind. To account for the amphistomatous nature of maize leaves (Driscoll et al., 2006), a correction factor is applied to the estimated g_b value (Müller et al., 2014). The corrected g_b value is then used to calculate C_b and e_b using A_{net}.

The energy balance submodel computes the steady-state leaf temperature (T_{leaf}) by balancing the fluxes of sensible heat, latent heat, and the energy consumed in photosynthesis with the radiation fluxes (Nikolov et al., 1995). The radiation fluxes consist of bidirectional absorbed PAR, NIR, and long-wave radiations and emitted long-wave radiation. The sensible heat (H) flux is computed using g_b (obtained from the boundary layer submodel) and the temperature between the leaf surface and its microenvironment. Latent heat flux (LE) is computed using the total conductance between leaf intercellular space and microenvironment obtained from the energy balance submodel (g) and water vapor gradient between leaf intercellular space and the microenvironment. While the sensible heat loss occurs equally from both sides of the leaf, latent heat loss is more on the abaxial surface than the adaxial surface due to the amphisotmatous nature of maize leaves.

2.2 | Model implementation

vLeaf is a MATLAB-based model that simultaneously solves the four leaf submodels to obtain steady-state fluxes of carbon, water, and energy from a C_4 leaf. The model is driven by leaf microenvironmental and biophysical parameter inputs and outputs leaf fluxes (carbon, water, energy) and states (temperature, conductance, C_i, etc.). To solve all four submodels simultaneously, vLeaf employs a Gauss-Seidel fixed-point iteration technique with a successive under-relaxation parameter of 0.8. The iteration loop is initialized with $C_i = 0.4C_a$, $A_{net} = 0.1C_a$, and $T_{leaf} = T_{air}$. The convergence criteria applied were $|\Delta C_i| < 0.01$, $|\Delta T_{leaf}| < 0.01$, and $|\Delta A_{net}| < 0.005$, where Δ denotes the error in the variable values between two successive iterations. vLeaf is implemented on a modular parallel computing driver platform to concurrently simulate multiple leaves, each within distinct microenvironments, making it computationally efficient.

While the mesophyll PEP carboxylation rate (V_p) in the photosynthesis sub-model can be solved directly, the Rubisco carboxylation rate (V_c) in the bundle sheath cells must be solved numerically. A_{net}, along with V_c, bundle sheath [O_2] (O_{bs}), and bundle sheath [CO_2] (C_{bs}), are obtained by simultaneously solving Equations: (S2), (S10), (S13), and (S14) using the *fminsearch* optimization algorithm (Lagarias et al., 1998). The error (sum of squares between successive iterations) tolerance for this optimization was set at 1E−4. Similarly, the solution for T_{leaf} is obtained by numerically solving the nonlinear energy balance equation (Equation: S32) using the *fminbnd* (bounded root finding algorithm) (Brent, 1973; Forsythe, 1977). The error (energy balance residual) tolerance for this optimization was set at 1E−4, with the upper and lower T_{leaf} bounds as 0° and 60°, respectively.

2.3 | g_s reduction simulations under varying microenvironmental conditions

g_s in leaves can be reduced through decreased stomatal size or density (Doheny et al., 2012; Franks et al., 2015). While g_s varies linearly with stomatal density, its relationship with stomatal size follows a square root dependence (Franks et al., 2009; Sack & Buckley, 2016). vLeaf simulates a reduction in stomatal size or density by decreasing the slope parameter (m) and the intercept parameter (b) of the Ball–Berry model. Due to the complex nonlinear interdependencies between the different leaf-level submodels, a 10% decrease in the SIP parameters does not necessarily translate to a 10% reduction in g_s or τ.

To study the impact of reducing g_s across diverse micro-environmental conditions, we conducted simulations by individually altering each microenvironmental variable from a reference base case. The base case conditions represent near optimal mid-day conditions experienced by fully expanded upper canopy leaves from a mature maize crop growing in the US Midwest corn belt (Table 1, upper leaves). The photosynthetic parameters of upper canopy maize leaves were obtained by fitting the model with measured data from field-grown maize plants (see Figure 3).

Lower leaves were assumed to be located at about 50% height from the top of a mature maize crop. Since the vertical distribution of leaf area in maize crops is relatively uniform (Boedhram et al., 2001), this roughly corresponds to the depth at which a maize canopy has 50% overlaying LAI. At this depth, the photosynthetic capacity of maize leaves is 37% of the upper canopy leaves (Drewry et al., 2010). The base-case incident shortwave radiations (PAR_i and NIR_i) and the wind speed (v) at this canopy depth were obtained using results from a multilayer canopy model (Drewry et al., 2010). The model assumes that the total long-wave radiation absorbed by upper canopy leaves consists of incoming long-wave radiation from the sky (top-half) and the surrounding lower leaves (bottom-half). The lower canopy leaves, on the other hand, receive long-wave radiation from surrounding upper (top-half) and lower (bottom-half) canopy leaves. The environmental conditions and the biophysical parameters for the lower canopy leaves are summarized in Table 1.

TABLE 1 Base-case leaf microenvironment inputs for upper and lower canopy C_4 maize leaves.

			Upper leaves	Lower leaves
Microenvironment inputs	$PPFD_i$	μmol m^{-2} s^{-1}	1750	350
	NIR_i	W m^{-2}	468	152
	C_a	ppm	420	420
	T_{air}	°C	25	25
	RH	%	70	70
	v	m s^{-1}	2	1
Photosynthetic parameters	$V_{c,max@25oC}$	μmol m^{-2} s^{-1}	55	20
	$J_{max@25oC}$	μmol m^{-2} s^{-1}	350	130
	$V_{p,max@25oC}$	μmol m^{-2} s^{-1}	110	40
	$V_{pr@25oC}$	μmol m^{-2} s^{-1}	80	30

Note: The incident and emitted long-wave radiations are modeled based on T_{air}, T_{leaf}, and e_a (Equation: S33).

The optimal g_s for beneficial tradeoffs in WUE was chosen such that a reduction in g_s did not induce a significant reduction in A_{net}. g_s reduction induces a sharp drop in A_{net} only when the PEP carboxylation switches from light-limited to CO_2-limited, that is, $A_p = A_{p,CO_2}$. This happens when $A_{p,Light} > A_{p,CO_2}$. Therefore, the optimal g_s reduction point at a given microenvironmental condition is chosen when $A_{p,Light} = A_{p,CO_2}$.

2.4 | Quantifying the primary and secondary effects of g_s reduction

The primary effect of g_s reduction is to decrease τ. Additionally, a reduction in τ decreases latent heat cooling of the leaf, thereby increasing T_{leaf} and sensible heat loss. However, increases in T_{leaf} can affect τ through secondary feedback of (i) increased vapor pressure gradient, (ii) modified photosynthetic enzyme activity, and (iii) modified leaf boundary layer conductance. The feedback resulting

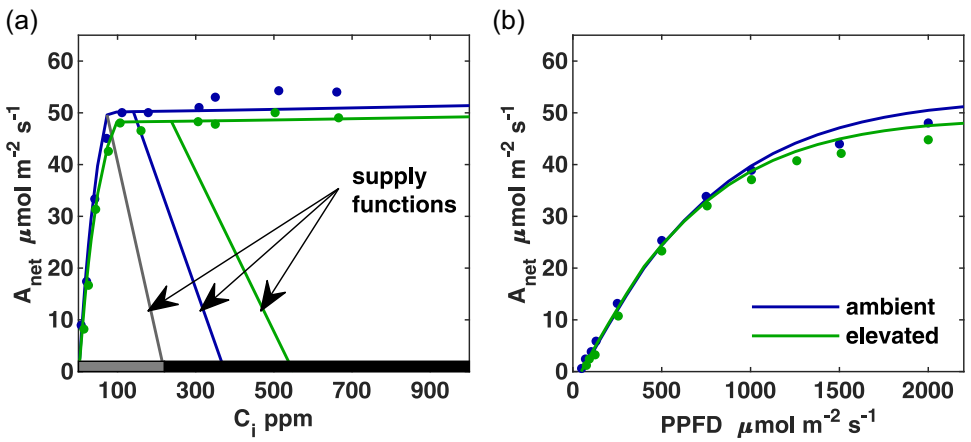

FIGURE 3 Model simulated (a) CO_2 (A-Ci) response and (b) light (A-Q) response of net CO_2 assimilation rates (A_{net}) at ambient (376 ppm solid blue) and elevated (550 ppm solid line) [CO_2], superimposed with measured data from maize leaves (Leakey et al., 2006). Horizontal gray and black bars in (a) represent regions with operating points in the initial slope and plateau regions of the A-Ci response, respectively. For both A-Ci and A-Q response simulations, air temperature (T_{air}) = 30° C, RH = 70%, incident long-wave was based on T_{air} (see Equation: S33) and $J_{max@25oC}$ = 350 μmol m^{-2} s^{-1}. For A-Ci response simulations the incident PPFD = 1750 μmol m^{-2} s^{-1}, $V_{p,max@25oC}$ = 110 (ambient), 95 (elevated) μmol m^{-2} s^{-1}, and $V_{c,max@25oC}$ = 60 (ambient), 55 (elevated) μmol m^{-2} s^{-1}. For the A-Q response simulations $V_{c,max@25oC}$ = 55 (ambient), 50 (elevated) μmol m^{-2} s^{-1}. Other leaf model parameters are given in Table S1. [Color figure can be viewed at wileyonlinelibrary.com]

from the increase in T_{leaf} is referred to as a secondary effect. vleaf model accounts for this secondary effect through the energy balance submodel.

To quantify and isolate the individual contributions of the primary and secondary effects of g_s reduction, three sets of simulations were performed using the same microenvironment inputs:

Case 1. Control simulation: no SIP reduction with energy balance turned on.
Case 2. Standard g_s reduction simulation: SIP reduction with energy balance turned on.
Case 3. Modified g_s reduction simulation: SIP reduction with energy balance turned off, and T_{leaf} was set to the value obtained under the control simulations (Case 1).

The standard g_s reduction simulation (Case 2) with energy balance captures both the primary and secondary effects. However, by forcing T_{leaf} in the modified g_s reduction simulations (Case 3) to be the same as that under the control simulations (Case 1), the secondary effects of g_s reduction due to increases in T_{leaf} are eliminated. Therefore, the modified g_s reduction simulation (Case 3) only quantifies the primary effect of g_s reduction. To isolate only the secondary effect of g_s reduction, we take the difference between the standard g_s reduction simulation (Case 2) and the modified g_s reduction simulation (Case 3). The set of these three simulations provides us with estimates of the primary effect, secondary effect, and combined primary and secondary effects of g_s reduction at the leaf level.

2.5 | g_s reduction simulations under current and future climate

To study the effect of g_s reduction on upper and lower canopy leaves under actual field conditions, model simulations were performed over the course of a typical diurnal period experienced by a mature maize crop in the US Midwest corn belt. The weather data for diurnal simulations was obtained from the SoyFACE research facility, situated on the south side of the University of Illinois Urbana-Champaign, IL, US (40°02′N, 88°14′ W, 228 m elevation) (Aspray et al., 2023; Meyers, 2016). The facility adopted a rotation practice of alternating soybean (even years) and maize (odd years) crops, with the weather station measuring the micro-meteorological conditions over a maize crop in odd years. A 10-year (2001–2021) average hourly micrometeorological variables were obtained from field measurements corresponding to the growing period of a fully mature maize crop between 190 and 220 Julian days (Boedhram et al., 2001) (Figure S1). The average diurnal data during this period was used as the microenvironment input for the upper canopy leaf. The diurnal microenvironment of the lower canopy was derived from the upper canopy by scaling the PAR, NIR, and wind speed using fixed ratios of the upper and lower canopy as outlined in Table 1.

Model simulations for future climate scenarios were performed under an elevated atmospheric $[CO_2]$ of 550 [ppm], representing the expected $[CO_2]$ in 2050 (Houghton et al., 2001). Additional effects of increased air temperatures (warmer climate with +2.7° C) and increased VPD (drier climate with −3.5% RH corresponding to +0.4 kPa VPD) were superimposed on elevated $[CO_2]$ simulations (DeLucia et al., 2019; Lobell et al., 2014; Pryor & Barthelmie, 2013). The inflection point in the A_{net}-SIP reduction relationship is defined as the optimal SIP reduction.

3 | RESULTS

3.1 | Model validation

vLeaf model was validated with data obtained from CO_2 (A-Ci) and light (A-Q) response measurements of field-grown maize under the then ambient (376 ppm in 2006) and future elevated (projected 550 ppm in 2050) $[CO_2]$ using free air concentration enrichment (FACE) technology (Leakey et al., 2006). Model simulations of A-Ci response under saturating light reproduced the biphasic behavior of C_4 leaves (Figure 3a). The model simulated A-Q response of maize leaves under ambient and elevated $[CO_2]$ reproduced the observed hyperbolic trajectory with diminishing gains in photosynthesis at higher light intensities (Figure 3b). Field-grown maize leaves do not show a significant photosynthetic acclimation effect at elevated $[CO_2]$ (Leakey et al., 2006). Therefore, we will use the photosynthetic parameters ($V_{c,max@}25°$ C, $V_{p,max@}25°$ C, $J_{max@}25°$ C) from the ambient A-Q response for the rest of the upper leaves simulation.

At the average $[CO_2]$ of the past half million years in which the ancestors of maize evolved, A_{net} under light-saturated conditions is limited by the initial slope of the A-Ci response (Figure 3a, gray horizontal bar). In contrast, at today's $[CO_2]$, A_{net} is determined by the A-Ci plateau (Figure 3a, blue supply function). In this plateau region where the operating C_i is greater than the C_i at the inflection point, there is no additional carbon gain with $[CO_2]$ increase (Figure 3a, black horizontal bar). Under future elevated $[CO_2]$, A_{net} remains constant, while g_s decreases (Figure 3a, green supply function) (Kollist et al., 2014; Leakey et al., 2006), causing τ to decrease, resulting in WUE gains. However, we can further reduce g_s under current and future elevated $[CO_2]$ such that the operating point is at (or near) the inflection point, resulting in even higher water savings without loss in photosynthesis. The following sections explore the tradeoffs in g_s reduction for upper and lower canopy leaves under varying leaf micro-environmental conditions.

3.2 | Quantifying the primary and secondary effects of g_s reduction

Using modified energy balance simulations (see Section 2.4), we quantify the contributions of primary and secondary effects of SIP reduction on A_{net}, τ, and WUE. We performed simulations on mature upper canopy leaves under ambient (420 ppm) and elevated (550 ppm) $[CO_2]$ for T_{air} of 25°C, 30°C, and 35° C. As expected, SIP reduction increases T_{leaf} across all $[CO_2]$ and T_{air} (Figure 4a,b).

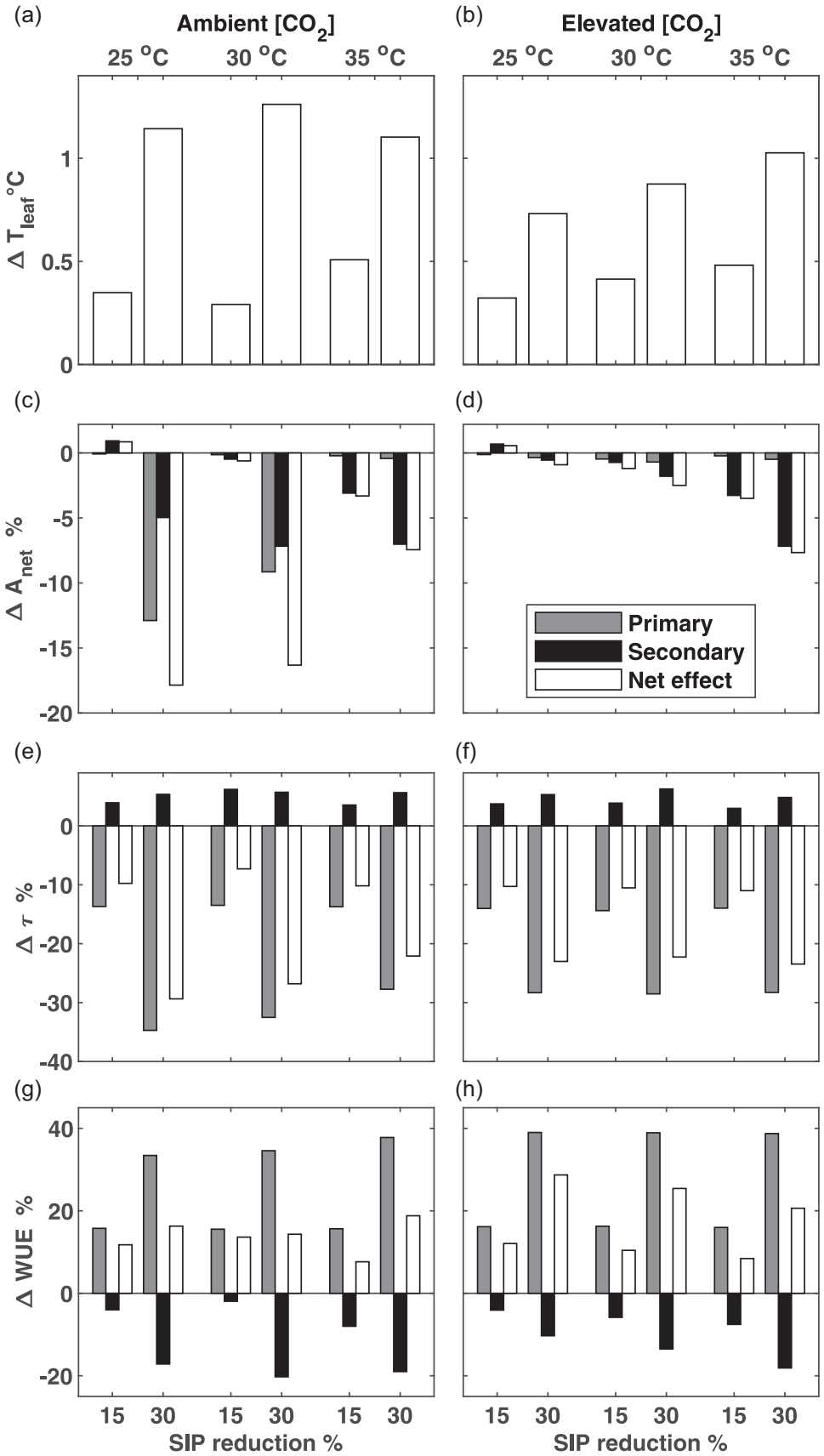

FIGURE 4 Model simulated primary and secondary effects of SIP reduction on percentage changes in (a and b) leaf temperature (ΔT_{leaf}), (c and d) photosynthesis (ΔA_{net}%), (e and f) transpiration ($\Delta\tau$%), and (g and h) WUE gains (ΔWUE%) under varying SIP reductions (15% and 30%), T_{air} (25°C, 30°C, and 35° C) and [CO_2] (ambient = 420 ppm and elevated = 550 ppm). The gray bar shows the primary effect, and the black bars show the secondary effects of SIP reduction. Simulations were performed on mature upper canopy leaves with model inputs in Table 1. Other model parameters are in Table S1.

Increases in T_{leaf} are higher under stronger SIP reductions and lower under higher $[CO_2]$. For the simulations considered, T_{leaf} increases are maximum (up to 1.26°C) under ambient $[CO_2]$, T_{air} of 30°C, and at 30% SIP reduction.

The primary effect of SIP reduction on photosynthesis is to decrease A_{net}. This decrease happens across all T_{air}, $[CO_2]$, and SIP reduction magnitudes (gray bars in Figure 4c,d). However, except for a 30% SIP reduction under ambient $[CO_2]$ (when the operating point shifts below the inflection point in the A-Ci response), the magnitudes of the primary effect on A_{net} are negligible (< 1%). The secondary effects of SIP reduction cause significant (up to 7%) additional loss in A_{net} when T_{air} > 30°C (temperature optimum for photosynthesis). Here, the secondary effect of temperature on photosynthetic enzyme kinetics and VPD act in sync to reduce A_{net}. When T_{air} = 25°C, the secondary effects marginally increase A_{net} at a 15% SIP reduction under ambient $[CO_2]$. However, for a 30% SIP reduction, there is a significant decrease in A_{net}. This is because, at a T_{air} = 25°C, the two secondary effects counteract each other, that is, while the effect of temperature on photosynthetic enzyme kinetics increases A_{net}, the secondary effects on VPD decrease A_{net}. Under ambient $[CO_2]$, VPD changes dominate the secondary effects at 30% SIP reduction, while under a 15% SIP reduction, the temperature effect on photosynthetic enzyme kinetics dominates the secondary effects (Figure 4c). At a T_{air} of 25°C, under a 30% SIP reduction, we observe a decrease in the secondary effect on A_{net} (Figure 4d). This is because elevated $[CO_2]$ partially offsets the detrimental VPD effect. The contribution of the secondary effects to the overall drop in A_{net} increases with increasing T_{air} and ranges between 27% and 95% as T_{air} increases from 25°C to 35°C (Figure 4c,d). Compared to elevated $[CO_2]$, SIP reduction's secondary effects on A_{net} are stronger under ambient $[CO_2]$.

The primary effect of SIP reduction on transpiration is to decrease τ across all T_{air}, $[CO_2]$, and SIP reduction magnitudes (gray bars in Figure 4e,f). These primary effects are higher under higher SIP reductions. The secondary effect of SIP reduction on τ always counteracts the primary effects and reduces the overall water savings across all T_{air}, $[CO_2]$, and SIP reduction magnitudes (black bars in Figure 4e,f). Higher SIP reductions increase the secondary effects. However, they are fairly constant under higher atmospheric $[CO_2]$. Overall, the secondary effects can diminish the water savings achieved through the primary effect by up to 6%. This trend was also reflected in the WUE gains (Figure 4g,h). While the primary effects of SIP reduction always increase WUE, the secondary effects always decrease WUE. The adverse impact of these secondary effects on WUE can be up to 20% (Figure 4g,h, black bars).

3.3 | g_s reduction under varying leaf microenvironment

Simulations were performed on C_4 maize leaves to assess the tradeoffs in g_s reduction under varying atmospheric $[CO_2]$, incident PPFD, RH, and T_{air}, under control (solid lines), 15% (dotted lines), and 30% SIP reduction (dashed lines) (Figures 5 and 6). Regions where SIP reduction causes an undesirable drop in A_{net} are shown in red (when PEP carboxylation switches from being light-limited to CO_2-limited, i.e., $A_{p,CO_2} < A_{p,Light}$).

3.3.1 | Upper canopy leaves

Model simulations under varying $[CO_2]$ show that, at ambient $[CO_2]$, while a 15% reduction in SIP does not cause any loss in A_{net}, it induces a 10% drop in τ, resulting in a 12% gain in WUE (Figure 5a–c dotted lines). However, while a 30% SIP reduction results in higher declines in τ (31%), the WUE gains are limited to 14% because of an undesirable 23% drop in A_{net} (Figure 5a–c, dashed line). This undesirable decline in A_{net} occurs due to a reduction in C_{bs} (Figure S2c) because PEP carboxylation rates are limited by CO_2 supply ($A_{p,CO_2} < A_{p,Light}$) (Figure S2a,b). At an atmospheric $[CO_2]$ > 590 ppm, PEP carboxylation rates switch from being CO_2-limited to light-limited for a 30% SIP reduction (Figure S2a), resulting in a 26% reduction in τ and a 29% gain in WUE without loss in A_{net} (Figure 4b,c). These simulations show that increasing $[CO_2]$ enhances the beneficial tradeoffs of g_s reduction in upper canopy leaves.

SIP reduction simulations performed under varying incident PPFD show that, at a 15% SIP reduction, A_{net} remains unaffected at all light levels. This results in a transpiration drop of 10%–12%, resulting in 12%–14% WUE gains (Figure 5d–f). Even at a 30% SIP reduction, A_{net} decreases only when incident PPFD >1279 μmol m^{-2} s^{-1} (Figure 5d) as PEP carboxylation rates switch from being light-limited to CO_2-limited (Figure S2d–f). When light levels are below this threshold PPFD of 1279 μmol m^{-2} s^{-1}, PEP carboxylation rates remain light-limited. Here, a 30% SIP reduction results in 21%–25% water savings and a 27%–33% gain in WUE, without any decline in A_{net} (Figure 5d–f). These results show that low-light conditions enhance g_s reduction's beneficial tradeoffs in upper canopy leaves.

Declines in RH induce stomatal closure, reducing g_s and shifting the operating point towards the inflection point of the A-Ci response (Figure S3). Even without SIP reduction, A_{net} declines when RH drops below 42%. This is because lower RH induces stomatal closure, restricting CO_2 supply to the mesophyll cell, thereby limiting PEP carboxylation rates ($A_{p,CO_2} < A_{p,Light}$) (Figure S2g,h). Under SIP reductions of 15% and 30%, A_{net} starts to decline at higher RH values of 61% and 92%, respectively (Figure 5g). Unlike A_{net}, which exhibits a threshold behavior with SIP reduction as RH varies, τ decreases with SIP reduction at all RH values (Figure 5h). These simulations show that beneficial tradeoffs of g_s reduction in upper canopy leaves diminish under lower RH values.

Across a range of air temperatures, a 15% SIP reduction does not cause any drop in A_{net} while inducing a 10%–12% reduction in τ, resulting in 9%–16% gains in WUE with higher WUE gains at lower T_{air} (Figure 5k,l, dotted lines). A_{net} decline is observed at 30% SIP reduction only when 13.25°C < T_{air} < 33.75°C. In this temperature range, PEP carboxylation is CO_2-limited rather than light-limited

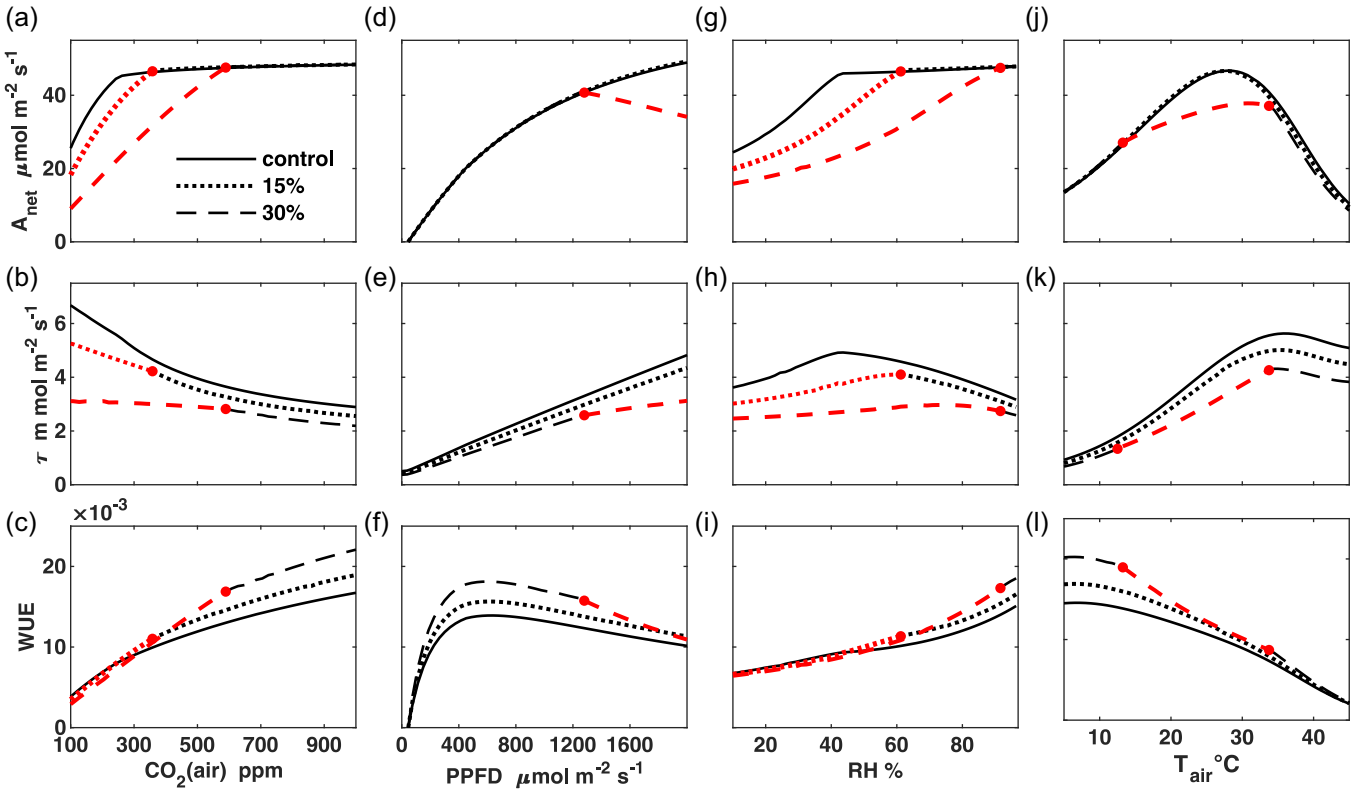

FIGURE 5 Model simulated variation of A_{net}, τ, and WUE in upper canopy leaves with atmospheric [CO_2] (a–c), incident PPFD (d–f), RH (g–i), and T_{air} (j–l) under SIP reductions of 0% (solid), 15% (dotted), and 30% (dashed). The region shown in red dots indicates where the tradeoffs in g_s reduction result in undesirable losses in A_{net}. Photosynthetic parameters and base case microenvironment data for upper canopy leaves are given in Table 1. Other model parameters are given in Table S1. [Color figure can be viewed at wileyonlinelibrary.com]

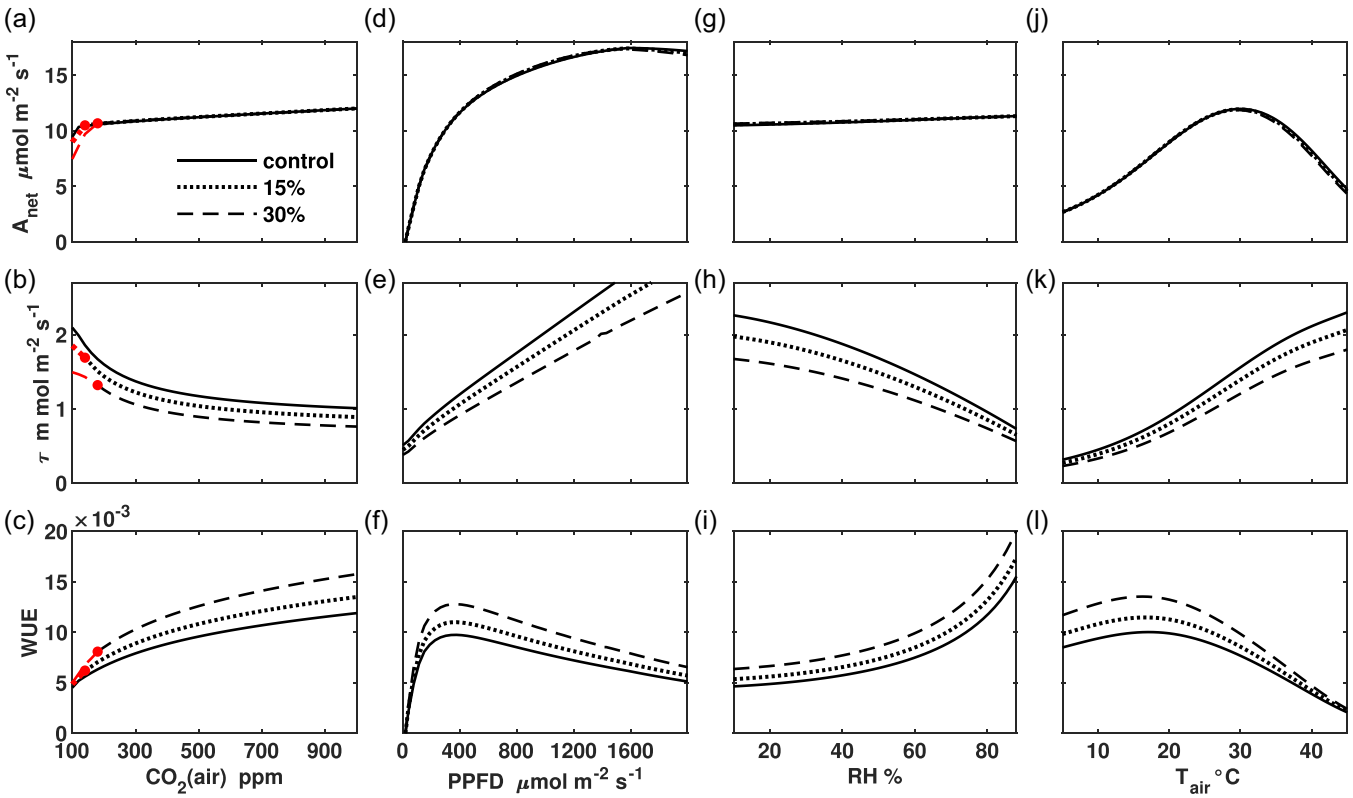

FIGURE 6 Same as Figure 5, but for lower canopy leaves. [Color figure can be viewed at wileyonlinelibrary.com]

(Figure S2j). For T_{air} of 30°C, a 15% SIP reduction results in 10% water savings without any drop in A_{net}, resulting in a 9% gain in WUE (Figure 5k,l). A 30% SIP reduction results in a higher water saving of 28%, but WUE gains are limited to 13% due to an undesirable 17% loss in A_{net} (Figure 5j–l). These simulations show that the beneficial tradeoffs of g_s reduction in upper canopy leaves are higher as the air temperatures diverge from the temperature optimum for photosynthesis. Note that reductions in SIP do not directly correspond to proportional reductions in g_s or τ (Figures S5 and S7). This is due to the presence of complex nonlinear feedback between the different leave submodels, which vary with microenvironmental conditions.

Wind speed influences g_b and, in turn, photosynthesis and transpiration. A higher wind speed increases $g_{b,forced}$, and hence g_b. Model simulations show that only when the wind speed is lower than 0.1 m s^{-1} (occurs less than 1% of the time in the US midwest) does $g_{b,forced}$ become smaller than $g_{b,free}$ (Figure S4a). Across a range of wind speeds, a 15% SIP reduction does not cause any drop in A_{net} while decreasing transpiration by 7%–11% and improving WUE by 8%–13% (Figure S5a–c). At lower wind speeds, A_{net} increases marginally while τ increases by up to 33%, resulting in lowered WUE for control and 15% SIP reductions. For a 30% SIP reduction, undesirable reductions in A_{net} are observed at all wind speed values with higher losses at lower wind speeds (Figure S5a–c). This is because at lower wind speeds, C_i decreases (Figure S4b), and since at 30% SIP reduction, A_{net} is limited by CO_2 supply ($A_{p,CO2} < A_{p,Light}$) (Figure S5d), a reduction in C_i results in declines in A_{net}. However, transpiration continues to increase with lower wind speed due to higher T_{leaf} (Figure S4c). These simulations show that the tradeoffs of g_s reduction in upper canopy leaves are beneficial across a range of wind speeds with increasing benefits at higher wind speed values.

3.3.2 | Lower canopy leaves

The CO_2 response of lower canopy leaves also exhibits a biphasic behavior, albeit with a diminished plateau (Marchiori et al., 2014; Pignon et al., 2017) due to lower incident PPFD and lower photosynthetic enzyme concentrations (Figure 6a and Table 1). The plateau region in lower canopy leaves has a mild slope such that A_{net} marginally increases with increasing [CO_2]. However, within this plateau, PEP carboxylation rates are limited by light, not CO_2, that is, $A_{p,Light} < A_{p,CO_2}$ (Figure S9a–c). In this plateau region, the tradeoffs in g_s reduction are still beneficial, albeit accompanied by a minor drop in A_{net}. While the inflection point in the CO_2 response of upper canopy leaves occurs at a C_a of 260 ppm, the inflection point of lower canopy leaves occurs at a much lower C_a of 120 ppm. This enables lower canopy leaves to withstand higher g_s reductions before negatively impacting the tradeoffs in SIP reduction. Unlike A_{net}, which remains unchanged under SIP reduction for [CO_2] > 180 ppm, a 15%–30% SIP reduction results in water savings of 11%–12% and 22%–25%, thereby leading to 11%–13% and 28%–32% gains in WUE, respectively (Figure 6b,c). These simulations show that compared to upper canopy leaves, the tradeoffs of g_s reduction in lower canopy leaves with lower photosynthetic capacities are enhanced, and elevated [CO_2] further amplifies these beneficial tradeoffs. Similar to upper canopy leaves, reducing SIPs in lower canopy leaves also resulted in proportional drops in g_s (Figure S8).

SIP reduction simulations on lower canopy leaves under varying light do not show any effect on A_{net} at all light levels (Figure 6d). However, τ decreases by ≈11% and 23%, increasing WUE by ≈13% and 31%, under SIP reductions of 15% and 30%, respectively (Figure 6e,f). Gains in WUE are maximum at a PPFD of about 300 µmol m^{-2} s^{-1}, which is close to the average light levels experienced at this lower canopy level (Table 1). Interestingly, even without SIP reduction, when PPFD exceeds 1580 µmol m^{-2} s^{-1}, lower canopy leaves exhibit CO_2-limited PEP carboxylation rates ($A_{p,CO_2} < A_{p,Light}$) (Figure S9d,e). However, a reduction in SIP (up to 30%) does not affect A_{p,CO_2}; thus, A_{net} rates do not drop with decreasing CO_2 supply rates (Figure S9d). This is because the A_{p,CO_2} in lower canopy leaves experiencing high incident PPFD are limited by enzyme concentrations (due to low leaf nitrogen content) and not CO_2 (substrate) concentrations. Below the threshold PPFD of 1580 µmol m^{-2} s^{-1}, PEP carboxylation rates are light-limited, that is, $A_{p,CO_2} > A_{p,Light}$ (Figure S9d). These simulations show that the tradeoffs in g_s reduction for lower canopy leaves are more desirable than upper canopy leaves across all light levels.

Contrary to upper canopy leaves, where the beneficial tradeoffs of SIP reduction diminish under drier air, RH does not impact g_s reduction tradeoffs in lower canopy leaves (Figure 6g–i). Even at a 30% SIP reduction, A_{net} shows no declines, while τ decreases by 22%–26% across a range of RH. This results in a WUE increase of 28%–37%, with higher gains under lower RH values (Figure 6i). Variations in T_{air} do not impact the A_{net} of lower canopy leaves even at SIP reductions up to 30% (Figure 6j). However, transpiratory water savings between 10%–13% and 22%–26%, resulting in WUE between 8%–15% and 20%–36%, are realized due to 15%–30% SIP reductions, respectively (lower gains observed at higher T_{air}) (Figure 6k,l). Variations in wind speed do not significantly affect the SIP tradeoffs in lower canopy leaves, with marginal increases in WUE at lower wind speeds (Figure S10). This is because lower canopy leaves with diminished photosynthetic capacities typically experience lower incident light levels, and CO_2 supply rarely influences their PEP carboxylation rates. These simulations suggest that the g_s reduction tradeoffs are retained and enhanced in lower canopy leaves across a range of RH and T_{air} values.

3.4 | g_s reduction tradeoffs over a diurnal period

Simulations performed on upper and lower canopy leaves of mature maize crops over a typical diurnal period in the US Midwest (Figure S1) show beneficial WUE tradeoffs due to g_s reduction (Figure 7). At a SIP reduction of 15%, the carbon gain over a day remains unchanged (<1%) while inducing a water savings of 11% and 12% resulting in WUE gains of 13% and 14% in upper and lower canopy leaves, respectively (Figure 7d–f). Under a 30% SIP

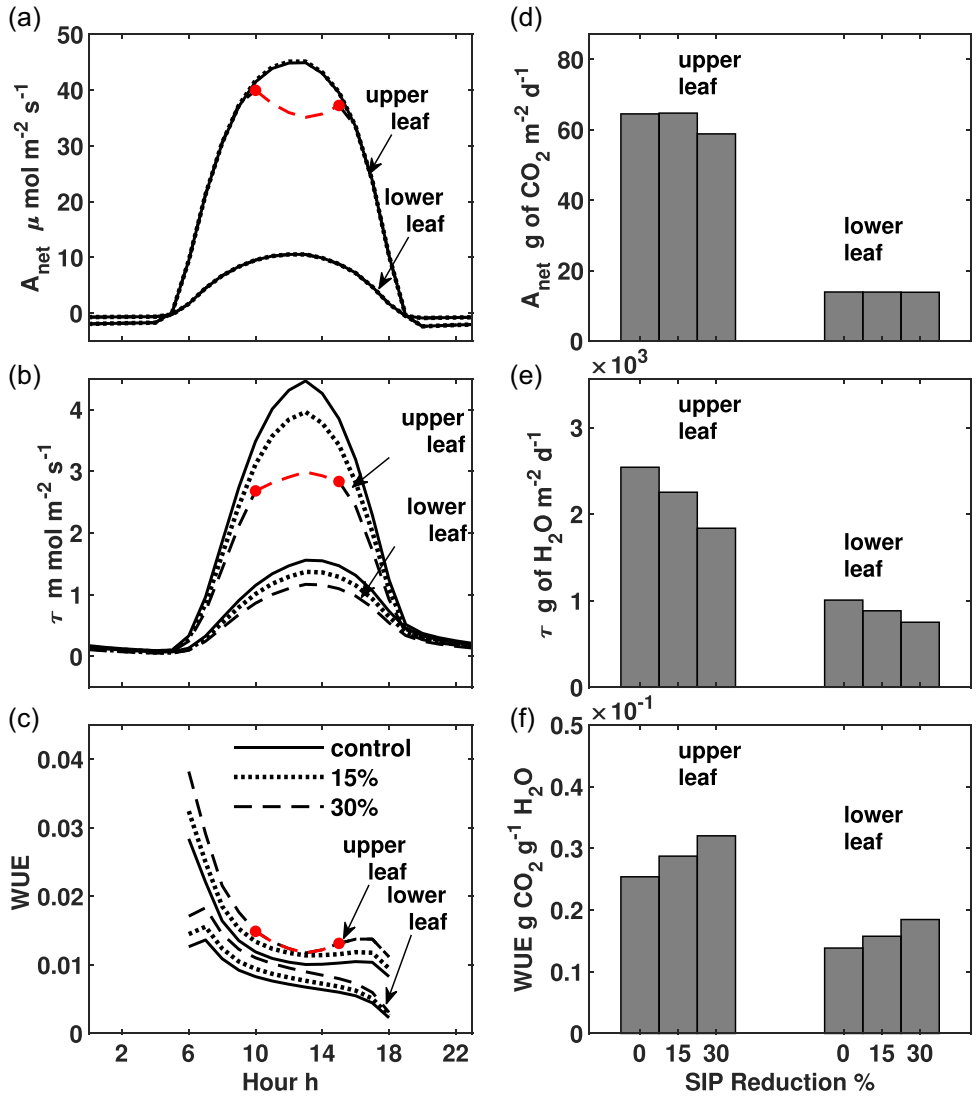

FIGURE 7 Model simulated diurnal variation in A_{net} (a), τ (b), WUE (c), and cumulative daily A_{net} (d), τ (e), and WUE (f) for upper and lower canopy leaves. Simulations were performed under SIP reductions of 0% (control), 15%, and 30%. The diurnal microenvironment of upper canopy leaves is obtained from Figure S1, and for lower canopy leaves, it was derived from the upper canopy by scaling the PAR, NIR, and wind speed using a fixed ratio between upper and lower canopy as outlined in Table 1 and Section 2.5. Photosynthetic parameters are given in Table 1. Other model parameters are given in Table S1. [Color figure can be viewed at wileyonlinelibrary.com]

reduction, while the A_{net} of lower canopy leaves is unchanged, upper canopy leaves experience an A_{net} drop of 10 μmol m^{-2} s^{-1} during a 5-h time window around mid-day (Figure 7a). In this time window, leaves experience higher incident light, lower RH, and higher air temperatures (Figure S1), conditions that are nonideal for SIP reduction. This mid-day drop of A_{net} results in only a 9% reduction in daily carbon gain (Figure 7d). Overall, a 30% SIP reduction produces water savings of 28% and 25%, resulting in WUE gains of 26% and 33% in upper and lower canopy leaves, respectively (Figure 7e,f). These simulations show that the tradeoffs associated with g_s reduction benefit both upper and lower canopy leaves over a typical diurnal period experienced by mature maize crops in the US Midwest.

3.5 | Optimal g_s reduction tradeoffs under current and future climate scenarios

Model simulations performed for a range of SIP reductions under current and projected mid-century future climatic conditions in the US Midwest show that the beneficial tradeoffs associated with SIP reductions are largely retained (Figure 8). Under current climate, the optimal SIP reduction for upper canopy leaves of mature maize crops is 22%. At this SIP reduction, for a <1% loss in carbon gain, a 17% water savings can be achieved, resulting in a 21% improvement in WUE (Figure 8, dashed black lines). Elevated [CO_2] increases the optimal SIP reduction of upper canopy leaves to 29%, resulting in a 32% improvement in WUE. This is because, under elevated [CO_2], the

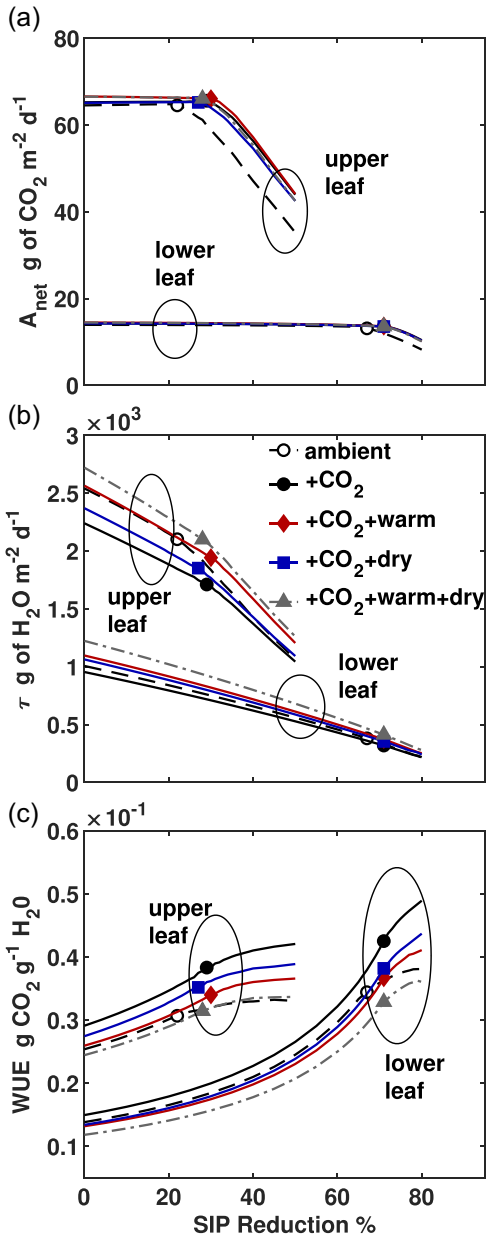

FIGURE 8 Model simulated variation in cumulative daily A_{net} (a), τ (b), and WUE (c) with SIP reduction under different climate conditions for upper and lower canopy leaves. Simulations for ambient climate are the same as Figure 7. Future climate scenarios in the US Midwest are simulated by offsetting the ambient weather data throughout the diurnal duration (Figure S1). Elevated [CO_2] (+CO_2) is obtained by increasing [CO_2] to 550 ppm. The warmer climate is represented by offsetting T_{air} by +2.7° C, and drier air is simulated by offsetting RH by −3.5% (absolute). Marker represents the optimal SIP reduction under the given climate scenario such that A_{net} remains unaffected due to SIP reduction while providing WUE gains (see Section 2.5 for more detail). Photosynthesis parameters are in Table 1, and other model parameters are in Table S1. [Color figure can be viewed at wileyonlinelibrary.com]

operating point shifts farther away from the inflection point of the A-Ci response, enabling higher SIP reductions and greater water savings (Figure 3a). WUE savings are preserved under future climates with elevated [CO_2] and warmer air temperatures. However, under a future climate with elevated [CO_2] and drier air, the optimal WUE gains drop to 28%. This is because drier air with lower RH decreases the SIP reduction potential (Figure S3). In summary, when considering the anticipated effects of future climate change, which include elevated [CO_2], warmer temperatures, and drier air, an optimal g_s reduction of 29% yields a 28% improvement in WUE (Figure 8, gray dash-dotted lines).

Lower canopy leaves with diminished photosynthetic capacities have a higher optimal SIP reduction (67%–71%) under current and future climatic conditions (Figure 8). This is because lower canopy leaves experience lower incident light, and their photosynthesis is typically light or enzyme limited and [CO_2]-saturated (Figure S9). This enhances the potential for g_s reduction without affecting photosynthetic rates. Therefore, the lower canopy leave's optimum SIP reduction potential shows less sensitivity to future climate variations (Figure S9). Under a future climate with elevated [CO_2], warmer temperature, and drier air, the optimal SIP reduction for lower canopy leaves is 71%, resulting in a dramatic 178% increase in WUE.

4 | DISCUSSION

Breeding and improved agronomy practices have achieved year-on-year increases in maize yields without reducing the water requirement per unit mass of biomass. Indeed, rising VPD would worsen this (Lobell et al., 2014; Ort & Long, 2014; Sinclair, 2018). However, rising atmospheric CO_2 allows easier access of CO_2 into the leaf, providing an apparent opportunity to breed for, or bioengineer, decreased stomatal conductance—lowering water loss without decreasing photosynthesis (Pignon & Long, 2020). The A-Ci response of maize leaves shows a biphasic nature. PEP carboxylase activity determines the initial slope and capacity for PEP regeneration, determining the plateau. The latter is assumed to be controlled by the activities of pyruvate Pi dikinase (PPDK) and ribulose-1:5 bisphosphate carboxylase/oxygenase (Rubisco) (Wang et al., 2020). The average [CO_2] of the last 420,000 years was 220 ppm (Wolff, 2005), the concentration at which we might assume our crop ancestors evolved. At this concentration, the operating point of maize photosynthesis is at the point of inflection between V_p (PEP carboxylation) and V_c (PEP regeneration), suggesting stomatal conductance is optimized to this past atmospheric [CO_2] (Figure 3a). Within a relatively short evolutionary time, [CO_2] has nearly doubled to 420 ppm today. Plants have probably not had time to fully adapt to this environmental change. As a result, the operating point has transitioned away from the optimal inflection point into the C_i-saturated plateau of the response. Future projected increases in atmospheric [CO_2] will further amplify this trend (Figure 3a).

Maize is the world's number one grain and crop in terms of production. While breeding, bioengineering, and agronomy have steadily increased yields, crop water use has also increased (Lobell et al., 2014; Long, 2014). With climate change expected to increase crop water demand and decrease freshwater availability, increases in crop yield will require simultaneous improvement in crop water use

efficiency (Kromdijk & Long, 2016; Ort & Long, 2014). While traditional crop breeding may have inadvertently increased stomatal conductance (Ainsworth & Long, 2005; Koester et al., 2016), maize germplasm exhibits significant variations in stomatal numbers, size, and conductance (Gleason et al., 2019; Xie et al., 2021), and researchers have identified genes that influence these traits (Lawson & Blatt, 2014; Lawson et al., 2011), suggesting the potential for engineering or breeding changes in conductance.

Past attempts to decrease g_s in C_3 plants such as legumes, rice, wheat, and so on, have also resulted in significant gains in WUE (Adams et al., 2018; Caine et al., 2019; Dunn et al., 2019; Franks et al., 2015; Hughes et al., 2017). However, the loss in A_{net} associated with these WUE gains does not show consistent trends across these studies. While some studies report gains in WUE without loss in photosynthesis (Adams et al., 2018; Dunn et al., 2019), others show that WUE gains are accompanied by significant undesirable declines in A_{net} (Caine et al., 2019; Franks et al., 2015; Hughes et al., 2017). While the photosynthesis of C_4 plants is CO_2 saturated, C_3 photosynthesis rates are not saturated at current and future elevated [CO_2]. Also, C_3 plants such as soybean show photosynthetic down-regulation acclimation response to increased [CO_2] (Bernacchi et al., 2005). A detailed modeling study of g_s reductions in C_3 plants can help understand the contrast in respose of different C_3 plants to g_s reduction.

Decreasing stomatal density in C_4 maize plants has shown decreased transpiration without loss in A_{net} under both control and drought conditions (Liu et al., 2014, 2015). However, optimal g_s reductions to avoid adverse impacts on photosynthesis rates due to the secondary effect of increased leaf temperature and VPD resulting from decreased latent heat from leaves with reduced g_s need to be known. Using a process-based coupled leaf-level model, we show that even when we account for the secondary effects, there is still a significant gain in WUE that would result from reduced g_s in the present and future elevated [CO_2] atmosphere. Previous studies primarily concentrated on the consequences of reducing g_s under saturating light, high RH, and controlled conditions. However, the current study highlights that this approach underestimates the potentially more significant benefits of the numerous shaded leaves within the dense canopies of modern maize crops. Our model results can help guide the development of crop phenotypes to achieve a sustainable, food-secure, and climate-resilient future.

The theoretical modeling analysis performed here considered optimal g_s reduction under nonwater-stressed conditions. When subject to water stress, C_4 leaves operating at optimal g_s will experience significant undesirable loss in A_{net} due to additional reductions in g_s. In reality, under natural conditions, leaves operating with a certain amount of redundancy will perform much better. This tradeoff between optimality and resilience has been explored in other crop optimization contexts (Leakey et al., 2019; Srinivasan, 2013; Srinivasan & Kumar, 2015). Therefore, the optimal SIP reduction will be dependent on other biotic and abiotic factors. Further studies are required to explore these aspects.

ACKNOWLEDGMENTS

This research was in part supported by the following grants: (i) Realizing Increased Photosynthetic Efficiency (RIPE) from the Bill & Melinda Gates Foundation, (ii) Foundation for Food and Agriculture Research (FFAR) and the UK Foreign, Commonwealth and Development Office, under grant number OPP1172157 (iii) CIE1819847N-FIGVENT and (iv) CE1920364NFSC008930 from the Center for Industrial Consultancy and Sponsored Research, Indian Institute of Technology Madras, (v) SB22230182CEPMRF008930 Prime Minister's Research Fellowship from the Department of Science and Technology, India, and (vi) the Early career grant ECR2018002762 from the Science and Engineering Research Board, Department of Science and Technology, India.

DATA AVAILABILITY STATEMENT

The code and parameters that have provided the results presented here are available at GitHub (will be made live on acceptance) https://github.com/ecohydrologylab/vLeaf

ORCID

Venkatraman Srinivasan http://orcid.org/0000-0003-4586-8893
Stephen P. Long http://orcid.org/0000-0002-8501-7164

REFERENCES

Adams, M.A., Buchmann, N., Sprent, J., Buckley, T.N. & Turnbull, T.L. (2018) Crops, nitrogen, water: are legumes friend, foe, or misunderstood ally? *Trends in Plant Science*, 23(6), 539–550. https://doi.org/10.1016/j.tplants.2018.02.009

Ainsworth, E.A. & Long, S.P. (2005) What have we learned from 15 years of free-air CO_2 enrichment (FACE)? A meta-analytic review of the responses of photosynthesis, canopy. *New Phytologist*, 165(2), 351–371. https://doi.org/10.1111/j.1469-8137.2004.01224.x

Aspray, E.K., Mies, T.A., McGrath, J.A., Montes, C.M., Dalsing, B., Puthuval, K.K. et al. (2023) Two decades of fumigation data from the soybean free air concentration enrichment facility. *Scientific Data*, 10(1), 226. https://doi.org/10.1038/s41597-023-02118-x

Ball, T.J., Woodrow, I.E. & Berry, J.A. (1987) A model predicting stomatal conductance and its contribution to the control of photosynthesis under different environmental conditions. *Progress in Photosynthesis Research*, 26(9), 1419–1430. https://doi.org/10.1007/978-94-017-0519-6_48

Bernacchi, C.J., Morgan, P.B., Ort, D.R. & Long, S.P. (2005) The growth of soybean under free air [co 2] enrichment (face) stimulates photosynthesis while decreasing in vivo rubisco capacity. *Planta*, 2203, 434–446. https://doi.org/10.1007/s00425-004-1320-8

Boedhram, N., Arkebauer, T.J. & Batchelor, W.D. (2001) Season-long characterization of vertical distribution of leaf area in corn. *Agronomy Journal*, 93(6), 1235–1242. https://doi.org/10.2134/agronj2001.1235

Brent, R.P. (1973) *Algorithms for minimization without derivatives*. Englewood Cliffs, NJ: Prentice-Hall.

Caine, R.S., Yin, X., Sloan, J., Harrison, E.L., Mohammed, U., Fulton, T. et al. (2019) Rice with reduced stomatal density conserves water and has improved drought tolerance under future climate conditions. *New Phytologist*, 221(1), 371–384. https://doi.org/10.1111/nph.15344

Campbell, G.S. & Norman, J.M. (1998) *An introduction to environmental biophysics*, 2nd ed. New York, NY: Springer.

Chan, S.S., Seidenfaden, I.K., Jensen, K.H. & Sonnenborg, T.O. (2021) Climate change impacts and uncertainty on spatiotemporal

variations of drought indices for an irrigated catchment. *Journal of Hydrology*, 601, 126814. https://doi.org/10.1016/j.jhydrol.2021.126814

Chen, D.X., Coughenour, M.B., Knapp, A.K. & Owensby, C.E. (1994) Mathematical simulation of C4 grass photosynthesis in ambient and elevated CO_2. *Ecological Modelling*, 73(1), 63–80. https://doi.org/10.1016/0304-3800(94)90098-1

Collison, R.F., Raven, E.C., Pignon, C.P. & Long, S.P. (2020) Light, not age, underlies the maladaptation of maize and miscanthus photosynthesis to self-shading. *Frontiers in Plant Science*, 11, 783. https://doi.org/10.3389/fpls.2020.00783

Cowan, I.R. & Farquhar, G.D. (1977) Stomatal function in relation to leaf metabolism and environment. In: Jennings, D.H. (Ed.) *Integration of activity in the higher plants. Symposia of the society of experimental biology*. Cambridge, UK: Cambridge University Press, pp. 471–505.

DeLucia, E.H., Chen, S., Guan, K., Peng, B., Li, Y., Nuria, G.C. et al. (2019) Are we approaching a water ceiling to maize yields in the United States? *Ecosphere*, 10(6), e02773. https://doi.org/10.1002/ecs2.2773

Doheny, A.T., Hunt, L., Franks, P.J., Beerling, D.J. & Gray, J.E. (2012) Genetic manipulation of stomatal density influences stomatal size, plant growth and tolerance to restricted water supply across a growth carbon dioxide gradient. *Philosophical Transactions of the Royal Society B: Biological Sciences*, 367(1588), 547–555. https://doi.org/10.1098/rstb.2011.0272

Drewry, D.T., Kumar, P., Long, S., Bernacchi, C., Liang, X.Z. & Sivapalan, M. (2010) Ecohydrological responses of dense canopies to environmental variability: 1. Interplay between vertical structure and photosynthetic pathway. *Journal of Geophysical Research-Biogeosciences*, 115(4), 1–25. https://doi.org/10.1029/2010jg001340

Drewry, D.T., Kumar, P. & Long, S.P. (2014) Simultaneous improvement in productivity, water use, and albedo through crop structural modification. *Global Change Biology*, 20(6), 1955–1967. https://doi.org/10.1111/gcb.12567

Driscoll, S.P., Prins, A., Olmos, E., Kunert, K.J. & Foyer, C.H. (2006) Specification of adaxial and abaxial stomata, epidermal structure and photosynthesis to CO2 enrichment in maize leaves. *Journal of Experimental Botany*, 57(2), 381–390. https://doi.org/10.1093/jxb/erj030

Dunn, J., Hunt, L., Afsharinafar, M., Meselmani, M.A.I., Mitchell, A., Howells, R. et al. (2019) Reduced stomatal density in bread wheat leads to increased water-use efficiency. *Journal of Experimental Botany*, 70(18), 4737–4748. https://doi.org/10.1093/jxb/erz248

FAO, IFAD, UNICEF, WFP and WHO (2021) *The state of food security and nutrition in the world 2021*. FAO. https://doi.org/10.4060/cb4474en

Faralli, M., Matthews, J. & Lawson, T. (2019) Exploiting natural variation and genetic manipulation of stomatal conductance for crop improvement. *Current Opinion in Plant Biology*, 49, 1–7. https://doi.org/10.1016/j.pbi.2019.01.003

Farquhar, G.D. & Sharkey, T.D. (1982) Stomatal conductance and photosynthesis. *Annual Review of Plant Physiology*, 33(1), 317–345. https://doi.org/10.1146/annurev.pp.33.060182.001533

Forsythe, G.E., Malcolm, M.A. & Moler, C.B. (1977) *Computer methods for mathematical computations*. Englewood Cliffs, NJ: Prentice-hall.

Franks, P.J., Doheny-Adams, T.W., Britton-Harper, Z.J. & Gray, J.E. (2015) Increasing water-use efficiency directly through genetic manipulation of stomatal density. *New Phytologist*, 207(1), 188–195. https://doi.org/10.1111/nph.13347

Franks, P.J., Drake, P.L. & Beerling, D.J. (2009) Plasticity in maximum stomatal conductance constrained by negative correlation between stomatal size and density: an analysis using *Eucalyptus globulus*. *Plant, Cell & Environment*, 32(12), 1737–1748. https://doi.org/10.1111/j.1365-3040.2009.002031.x

Franks, P.J. & Farquhar, G.D. (2007) The mechanical diversity of stomata and its significance in fas-exchange control. *Plant Physiology*, 143(1), 78–87. https://doi.org/10.1104/pp.106.089367

Gleason, S.M., Cooper, M., Wiggans, D.R., Bliss, C.A., Romay, M.C., Gore, M.A. et al. (2019) Stomatal conductance, xylem water transport, and root traits underpin improved performance under drought and well-watered conditions across a diverse panel of maize inbred lines. *Field Crops Research*, 234, 119–128. https://doi.org/10.1016/j.fcr.2019.02.001

Grossiord, C., Buckley, T.N., Cernusak, L.A., Novick, K.A., Poulter, B., Siegwolf, R.T.W. et al. (2020) Plant responses to rising vapor pressure deficit. *New Phytologist*, 226(6), 1550–1566. https://doi.org/10.1111/nph.16485

Hatch, M.D. (1987) C4 photosynthesis: a unique elend of modified biochemistry, anatomy and ultrastructure. *Biochimica et Biophysica Acta (BBA)—Reviews on Bioenergetics*, 895(2), 81–106. https://doi.org/10.1016/S0304-4173(87)80009-5.

Hetherington, A.M. & Woodward, F.I. (2003) The role of stomata in sensing and driving environmental change. *Nature*, 424(6951), 901–908. https://doi.org/10.1038/nature01843

Houghton, J.T., Ding, Y.D.J.G., Griggs, D.J., Noguer, M., van der Linden, P.J., Dai, X. et al. (2001) Climate change 2001.

Hughes, J., Hepworth, C., Dutton, C., Dunn, J.A., Hunt, L., Stephens, J. et al. (2017) Reducing stomatal density in barley improves drought tolerance without impacting on yield. *Plant physiology*, 174(2), 776–787. https://doi.org/10.1104/pp.16.01844

IPCC. (2014) *Climate change 2014: synthesis report*. Contribution of working groups I, II and III to the fifth assessment report of the intergovernmental panel on climate change. Technical report, Intergovernmental Panel on Climate Change.

Kimm, H., Guan, K., Gentine, P., Wu, J., Bernacchi, C.J., Sulman, B.N. et al. (2020) Redefining droughts for the US corn belt: The dominant role of atmospheric vapor pressure deficit over soil moisture in regulating stomatal behavior of maize and soybean. *Agricultural and Forest Meteorology*, 287, 107930. https://doi.org/10.1016/j.agrformet.2020.107930

Koester, R.P., Nohl, B.M., Diers, B.W. & Ainsworth, E.A. (2016) Has photosynthetic capacity increased with 80 years of soybean breeding? An examination of historical soybean cultivars. *Plant, cell & environment*, 39(5), 1058–1067. https://doi.org/10.1111/pce.12675

Kollist, H., Nuhkat, M. & Roelfsema, M.R.G. (2014) Closing gaps: linking elements that control stomatal movement. *New Phytologist*, 203(1), 44–62. https://doi.org/10.1111/nph.12832

Kromdijk, J. & Long, S.P. (2016) One crop breeding cycle from starvation? How engineering crop photosynthesis for rising CO_2 and temperature could be one important route to alleviation. *Proceedings of the Royal Society of London. Series B, Biological Sciences*, 283(1826), 20152578. https://doi.org/10.1098/rspb.2015.2578

Lagarias, J.C., Reeds, J.A., Wright, M.H. & Wright, P.E. (1998) Convergence properties of the Nelder-Mead simplex method in low dimensions. *SIAM Journal on optimization*, 9(1), 112–147. https://doi.org/10.1137/S1052623496303470.

Lawson, T. & Blatt, M.R. (2014) Stomatal size, speed, and responsiveness impact on photosynthesis and water use efficiency. *Plant Physiology*, 164(4), 1556–1570. https://doi.org/10.1104/pp.114.237107

Lawson, T. & Matthews, J. (2020) Guard cell metabolism and stomatal function. *Annual Review of Plant Biology*, 71(1), 273–302. https://doi.org/10.1146/annurev-arplant-050718-100251

Lawson, T., vonCaemmerer, S. & Baroli, I. (2011) Photosynthesis and stomatal behaviour. In: Houghton, J.T., Ding, Y., Griggs, D.J., Noguer, M., van der Linder, P.J., Dai, X., Maskell, K. & Johnson, C.A. (Eds.) *Progress in botony*, Vol. 72. Berlin: Springer-Verlag, pp. 265–304.

Leakey, A.D.B., Ferguson, J.N., Pignon, C.P., Wu, A., Jin, Z., Hammer, G.L. et al. (2019) Water use efficiency as a constraint and target for improving the resilience and productivity of C3 and C4 crops. *Annual Review of Plant Biology*, 70(1), 781–808. https://doi.org/10.1146/annurev-arplant-042817-040305

Leakey, A.D.B., Uribelarrea, M., Ainsworth, E.A., Naidu, S.L., Rogers, A., Ort, D.R. et al. (2006) Photosynthesis, productivity, and yield of maize are not affected by open-air elevation of CO_2 concentration in the absence of drought. *Plant Physiology*, 140(2), 779–790. https://doi.org/10.1104/pp.105.073957

Leuning, R. (1990) Modelling stomatal behaviour and and photosynthesis of *Eucalyptus grandis*. *Functional Plant Biology*, 17(2), 159–175. https://doi.org/10.1071/PP9900159

Leuning, R., Kelliher, F.M., De Pury, D. G.G. & Schulze, E.D. (1995) Leaf nitrogen, photosynthesis, conductance and transpiration: Scaling from leaves to canopies. *Plant, Cell & Environment*, 18(10), 1183–1200. https://doi.org/10.1111/j.1365-3040.1995.tb00628.x

Liu, Y., Han, L., Qin, L. & Zhao, D. (2014) *Saccharomyces cerevisiae* gene TPS1 improves drought tolerance in *Zea mays* L. by increasing the expression of SDD1 and reducing stomatal density. *Plant Cell, Tissue and Organ Culture (PCTOC)*, 120(2), 779–789. https://doi.org/10.1007/s11240-014-0647-5.

Liu, Y., Qin, L., Han, L., Xiang, Y. & Zhao, D. (2015) Overexpression of maize SDD1 (ZmSDD1) improves drought resistance in *Zea mays* L. by reducing stomatal density. *Plant Cell, Tissue and Organ Culture (PCTOC)*, 122(1), 147–159. https://doi.org/10.1007/s11240-015-0757-8

Lobell, D.B., Hammer, G.L., McLean, G., Messina, C., Roberts, M.J. & Schlenker, W. (2013) The critical role of extreme heat for maize production in the United States. *Nature Climate Change*, 3(5), 497–501. https://doi.org/10.1038/NCLIMATE1832

Lobell, D.B., Roberts, M.J., Schlenker, W., Braun, N., Little, B.B., Rejesus, R.M. et al. (2014) Greater sensitivity to drought accompanies maize yield increase in the US midwest. *Science*, 344(6183), 516–519. https://doi.org/10.1126/science.1251423

Long, S.P. (2014) We need winners in the race to increase photosynthesis in rice, whether from conventional breeding, biotechnology or both. *Plant Cell and Environment*, 37(1), 19–21. https://doi.org/10.1111/pce.12193

Long, S.P., Taylor, S.H., Burgess, S.J., Carmo-Silva, E., Lawson, T., Souza, A.P.D. et al. (2022) Into the shadows and back into sunlight: photosynthesis in fluctuating light. *Annual Review of Plant Biology*, 73(1), 617–648. https://doi.org/10.1146/annurev-arplant-070221-024745

Maherali, H.C.D.R., Reid, C.D., Polley, H.W., Johnson, H.B. & Jackson, R.B. (2002) Stomatal acclimation over a subambient to elevated CO2 gradient in a C3/C4 grassland. *Plant, Cell & Environment*, 25(4), 557–566. https://doi.org/10.1046/j.1365-3040.2002.00832.x

Marchiori, P.E.R., Machado, E.C. & Ribeiro, R.V. (2014) Photosynthetic limitations imposed by self-shading in field-grown sugarcane varieties. *Field Crops Research*, 155, 30–37. https://doi.org/10.1016/j.fcr.2013.09.025

Massad, R.S., Tuzet, A. & Bethenod, O. (2007) The effect of temperature on C4-type leaf photosynthesis parameters. *Plant Cell and Environment*, 30(9), 1365–3040. https://doi.org/10.1111/j.1365-3040.2007.01691.x

Meyers, T. (2016) AmeriFlux AmeriFlux US-Bo1 Bondville.

Morgan, P.B., Bernacchi, C.J., Ort, D.R. & Long, S.P. (2004) An in vivo analysis of the effect of season-long open-air elevation of ozone to anticipated 2050 levels on photosynthesis in soybean. *Plant Physiology*, 135(4), 2348–2357. https://doi.org/10.1104/pp.104.043968

Mü ller, J., Eschenröder, A. & Christen, O. (2014) LEAFC3-N photosynthesis, stomatal conductance, transpiration and energy balance model: finite mesophyll conductance, drought stress, stomata ratio, optimized solution algorithms, and code. *Ecological modelling*, 290, 134–145. https://doi.org/10.1016/j.ecolmodel.2013.10.036

Nagaraj, D., Proust, E., Todeschini, A., Rulli, M.C. & D'Odorico, P. (2021) A new dataset of global irrigation areas from 2001 to 2015. *Advances in Water Resources*, 152, 1039. https://doi.org/10.1016/j.advwatres.2021.103910

Nikolov, N.T., Massman, W.J. & Schoettle, A.W. (1995) Coupling biochemical and biophysical processes at the leaf level: an equilibrium photosynthesis model for leaves of C3 plants. *Ecological Modelling*, 80(2), 205–235. https://doi.org/10.1016/0304-3800(94)00072-P

Ort, D.R. & Long, S.P. (2014) Limits on yields in the corn belt. *Science*, 344(6183), 483–484. https://doi.org/10.1126/science.1253884

Pearcy, R.W. (1990) Sunflecks and photosynthesis in plant canopies. *Annual Review of Plant Physiology and Plant Molecular Biology*, 41(1), 421–453. https://doi.org/10.1146/annurev.pp.41.060190.002225

Phetluan, W., Wanchana, S., Aesomnuk, W., Adams, J., Pitaloka, M.K., Ruanjaichon, V. et al. (2023) Candidate genes affecting stomatal density in rice (*Oryza sativa* L.) identified by genome-wide association. *Plant Science*, 330, 111624. https://doi.org/10.1016/j.plantsci.2023.111624

Pignon, C.P., Jaiswal, D., McGrath, J.M. & Long, S.P. (2017) Loss of photosynthetic efficiency in the shade. an achilles heel for the dense modern stands of our most productive c4 crops? *Journal of Experimental Botany*, 68(2), 335–345. https://doi.org/10.1093/jxb/erw456

Pignon, C.P. & Long, S.P. (2020) Retrospective analysis of biochemical limitations to photosynthesis in 49 species: C4 crops appear still adapted to pre-industrial atmospheric [CO_2]. *Plant, Cell & Environment*, 43, 2606–2622. https://doi.org/10.1111/pce.13863

Pitaloka, M.K., Caine, R.S., Hepworth, C., Harrison, E.L., Sloan, J., Chutteang, C. et al. (2022) Induced genetic variations in stomatal density and size of rice strongly affects water use efficiency and responses to drought stresses. *Frontiers in Plant Science* 13, 13. https://doi.org/10.3389/fpls.2022.801706

Pryor, S.C. & Barthelmie, R.J. (2013) *The midwestern United States: socioeconomic context and physical climate*. Bloomington, IN: Indiana University Press, pp. 12–47. http://www.jstor.org/stable/j.ctt16gzks0.7

Sack, L. & Buckley, T.N. (2016) The developmental basis of stomatal density and flux. *Plant Physiology*, 171(4), 2358–2363. https://doi.org/10.1104/pp.16.00476

Sinclair, T.R. (2018) Effective water use required for improving crop growth rather than transpiration efficiency. *Frontiers in Plant Science*, 9, 1442. https://doi.org/10.3389/fpls.2018.01442

Srinivasan, V. (2013) *Optimality and resilience in patterns of carbon allocation and growth in vegetation under acclimation response to climate change* (PhD thesis).

Srinivasan, V. & Kumar, P. (2015) Emergent and divergent resilience behavior in catastrophic shift systems. *Ecological Modeling*, 298(SI), 87–105. https://doi.org/10.1016/j.ecolmodel.2013.12.003

Srinivasan, V., Kumar, P. & Stephen, P.L. (2016) Decreasing, not increasing, leaf area will raise crop yields under global atmospheric change. *Global Change Biology*, 23(4), 1626–1635. https://doi.org/10.1111/gcb.13526

Sulman, B.N., Roman, D.T., Yi, K., Wang, L., Phillips, R.P. & Novick, K.A. (2016) High atmospheric demand for water can limit forest carbon uptake and transpiration as severely as dry soil. *Geophysical Research Letters*, 43(18), 9686–9695. https://doi.org/10.1002/2016GL069416

Tilman, D. & Clark, M. (2015) Food, agriculture & the environment: can we feed the world and save the earth? *DAEDALUS*, 144(4), 8–23. https://doi.org/10.1162/DAED_a_00350

UNESCO. (2001) *Securing the food supply Paris*. Report, United Nations Educational, Scientific and Cultural Organization.

von Caemmerer, S. (2000) *Biochemical models of leaf photosynthesis. Techniques in plant sciences*. CISRO. https://doi.org/10.1071/9780643103405

von Caemmerer, S. & Furbank, R.T. (1999) Modeling C4 photosynthesis. In: Sage, R.F. & Monson, R.K. (Eds.) *C4 plant biology*. Academic Press, pp. 173–211.

Wang, Y., Burgess, S.J., de Becker, E.M. & Long, S.P. (2020) Photosynthesis in the fleeting shadows: an overlooked opportunity for increasing crop productivity? *The Plant Journal*, 101(4), 874–884. https://doi.org/10.1111/tpj.14663

Wolff, E.W. (2005) Understanding the past-climate history from Antarctica. *Antarctic Science*, 17(4), 487–495. https://doi.org/10.1017/S0954102005002919.

Xie, J., Fernandes, S.B., Mayfield-Jones, D., Erice, G., Choi, M., Lipka, E.A. et al. (2021) Optical topometry and machine learning to rapidly phenotype stomatal patterning traits for maize QTL mapping. *Plant Physiology*, 187(3), 1462–1480. https://doi.org/10.1093/plphys/kiab299

Yuan, W., Zheng, Y., Piao, S., Ciais, P., Lombardozzi, D., Wang, Y. et al. (2019) Increased atmospheric vapor pressure deficit reduces global vegetation growth. Science Advances, 5(8), eaax1396. https://doi.org/10.1126/sciadv.aax1396

SUPPORTING INFORMATION

Additional supporting information can be found online in the Supporting Information section at the end of this article.

How to cite this article: Srivastava, A., Srinivasan, V. & Long, S.P. (2024) Stomatal conductance reduction tradeoffs in maize leaves: A theoretical study. *Plant, Cell & Environment*, 1–16. https://doi.org/10.1111/pce.14821